Functionalized Macrocyclic Ligands for Use in Supramolecular Chemistry

Katie Campbell, Robert McDonald, and Rik R. Tykwinski*

Department of Chemistry, University of Alberta, Edmonton AB T6G 2G2, Canada

rik.tykwinski@ualberta.ca

Received July 27, 2001

The synthesis of three cross-conjugated macrocycles bearing pyridine functionality is described. The ability of two of these molecules, **5a** and **5c**, to behave as 4,4′-bipyridine mimics in self-assembly reactions is demonstrated by axial coordination to a metalloporphyrin. The directed coordinative ability of the pyridine rings ensures predictable self-assembly into well-ordered nanoscale systems, both in solution and the solid state. ^{1}H, ^{13}C, and HMQC NMR spectroscopic experiments and ESI MS have been used to characterize the supramolecular complexes in solution. X-ray crystallographic analysis of solid-state assemblies **7a** and **7c** provides insight into the scope and flexibility of these macrocyclic ligands as supramolecular building blocks. UV−vis and fluorescence spectroscopies provide a description of their electronic characteristics.

Introduction

Carbon-rich, conjugated macrocycles are of considerable interest due to their potential as new materials with shape persistent structures and desirable physical properties. Particularly appealing is the "tunability" of the physical characteristics of these highly conjugated scaffolds.[1] Through the covalent incorporation of functional groups, their structures can be manipulated to provide desirable physical properties tailored for specific applications. For example, coordinative functionality such as the nitrogen(s) of pyridine or bipyridine, directed toward the interior of macrocycles has been used in the design of artificial receptors[2] and ion sensors.[3]

We became intrigued by the idea of introducing functionality into a macrocyclic framework to provide a system capable of binding to metals and/or metal ions. Specifically, the incorporation of pyridine(s) such that the nitrogen(s) are directed away from the cyclic core could afford a ligand that, while still possessing the attributes of a cross-conjugated macrocycle, could also participate in self-assembly reactions.[4,5] Such a ligand could provide a variety of new hybrid architectures that feature metal atoms linked by a conjugated, porous macrocycle. Examination of recent literature reveals that bipyridines and related molecules are among the most widely used constituents[6] of supramolecular assemblies, due in part to their rigidity and directed coordinative ability. This is particularly true of 4,4′-bipyridine,[7] which is frequently employed toward the realization of discrete, highly ordered nanostructures based on transition metal coordination. Ligands **5a**−**c**, based on a 3,5-diethynyl pyridine building block, were therefore designed with the expectation that they could function as 4,4′-bipyridine analogues. The directed, exocyclic orientation of the pyridyl nitrogens ensures their predictable assembly into well-defined supramolecular scaffolds. Unlike bipyridines, however, the targeted macrocycles could potentially provide for the formation of porous solid-state structures (Figure 1).[8]

We demonstrate the coordinative ability of macrocycles **5a**−**c** via axial coordination to metalloporphyrin **6a** to give the corresponding assemblies **7a**−**c**.[9] These structures were targeted due to the widespread interest in

(1) (a) Marsella, M. J.; Wang, Z.-Q.; Reid, R. J.; Yoon, K. *Org. Lett.* **2001**, *3*, 885−887. (b) Mena-Osteritz, E.; Bäuerle, P. *Adv. Mater.* **2001**, *13*, 243−246. (c) Nakamura, K.; Okubo, H.; Yamaguchi, M. *Org. Lett.* **2001**, *3*, 1097−1099. (d) Höger, S.; Bonrad, K.; Mourran, A.; Beginn, U.; Möller, M. *J. Am. Chem. Soc.* **2001**, *123*, 5651−5659. (e) Sun, S.-S.; Lees, A. J. *J. Am. Chem. Soc.* **2000**, *122*, 8956−8967. (f) Tobe, Y.; Fujii, T.; Matsumoto, H.; Tsumuraya, K.; Noguchi, D.; Nakagawa, N.; Sonoda, M.; Naemura, K.; Achiba, Y.; Wakabayashi, T. *J. Am. Chem. Soc.* **2000**, *122*, 1762−1775. (g) Ohkita, M.; Ando, K.; Suzuki, T.; Tsuji, T. *J. Org. Chem.* **2000**, *65*, 4385−4390. (h) Collins, S. K.; Yap, G. P. A.; Fallis, A. G. *Org. Lett.* **2000**, *2*, 3189−3192. (i) Ge, P.-H.; Fu, W.; Herrmann, W. A.; Herdtweck, E.; Campana, C.; Adams, R. D.; Bunz, U. H. F. *Angew. Chem., Int. Ed.* **2000**, *39*, 3607−3610. (j) Eisler, S.; Tykwinski, R. R. *Angew. Chem., Int. Ed.* **1999**, *38*, 1940−1943. (k) Kawase, T.; Hosokawa, Y.; Kurata, H.; Oda, M. *Chem. Lett.* **1999**, 745−746. (l) Moore, J. S. *Acc. Chem. Res.* **1997**, *30*, 402−413. (m) Nielsen, M. B.; Schreiber, M.; Baek, Y. G.; Seiler, P.; Lecomte, S.; Boudon, C.; Tykwinski, R. R.; Gisselbrecht, J.-P.; Gramlich, V.; Skinner, P. J.; Bosshard, C.; Günter, P.; Gross, M.; Diederich, F. *Chem. Eur. J.* **2001**, *7*, 3263−3280.

(2) (a) Nitschke, J. R.; Tilley, T. D. *Angew. Chem., Int. Ed.* **2001**, *40*, 2142−2145. (b) Henze, O.; Lentz, D.; Schlüter, A. D. *Chem. Eur. J.* **2000**, *6*, 2362−2367. (c) Tobe, Y.; Nagano, A.; Kawabata, K.; Sonoda, M.; Naemura, K. *Org. Lett.* **2000**, *2*, 3265−3268. (d) Inouye, M.; Miyake, T.; Furusyo, M.; Nakazumi, H. *J. Am. Chem. Soc.* **1995**, *117*, 12416−12425.

(3) Baxter, P. N. W. *J. Org. Chem.* **2001**, *66*, 4170−4179.

(4) Campbell, K.; McDonald, R.; Branda, N. R.; Tykwinski, R. R. *Org. Lett.* **2001**, *3*, 1045−1048.

(5) Sun, S.-S.; Lees, A. J. *Organometallics* **2001**, *20*, 2353−2358.

(6) (a) Holliday, B. J.; Mirkin, C. A. *Angew. Chem., Int. Ed.* **2001**, *40*, 2022−2043. (b) Leininger, S.; Olenyuk, B.; Stang, P. J. *Chem. Rev.* **2000**, *100*, 853−908. (c) Fujita, M. *Chem. Soc. Rev.* **1998**, *27*, 417−425. (d) Philp, D.; Stoddart, J. F. *Angew. Chem., Int. Ed. Engl.* **1996**, *35*, 1154−1196. (e) Ziessel, R.; Suffert, J.; Youinou, M.-T. *J. Org. Chem.* **1996**, *61*, 6535−6546.

(7) (a) Manimaran, B.; Rajendran, T.; Lu, Y.-L.; Lee, G.-H.; Peng, S.-M.; Lu, K.-L. *J. Chem. Soc., Dalton Trans.* **2001**, 515−517. (b) Zaworotko, M. J. *Angew. Chem., Int. Ed.* **2000**, *39*, 3052−3054. (c) Dong, Y.-B.; Smith, M. D.; zur Loye, H.-C. *Inorg. Chem.* **2000**, *39*, 4927−4935.

(8) Sun, W.-Y.; Fan, J.; Okamura, T.-a.; Xie, J.; Yu, K.-B.; Ueyama, N. *Chem. Eur. J.* **2001**, *7*, 2557−2562. Biradha, K.; Aoyagi, M.; Fujita, M. *J. Am. Chem. Soc.* **2000**, *122*, 2397−2398. Aoyagi, M.; Biradha, K.; Fujita, M. *Bull. Chem. Soc. Jpn.* **1999**, *72*, 2603−2606. Choi, H. J.; Suh, M. P. *J. Am. Chem. Soc.* **1998**, *120*, 10622−10628. Fujita, M.; Ogura, K. *Bull. Chem. Soc. Jpn.* **1996**, *69*, 1471−1482. Moore, J. S. *Nature* **1995**, *374*, 495−496.

10.1021/jo0159744 CCC: $22.00
Published on Web 01/26/2002

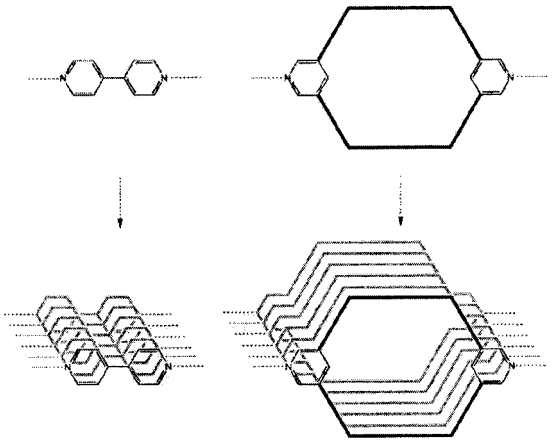

Figure 1. Schematic comparison of 4,4′-bipyridine and the targeted macrocycle as supramolecular building blocks.

multiporphyrin architectures, in addition to the well-established photophysical features of porphyrins.[10] X-ray crystallographic analysis of **7a** verifies the ability of these macrocycles to form highly ordered crystalline materials, whereas single-crystal X-ray analysis of **7c** establishes the flexibility of these macrocyclic ligands. The ability of the macrocyclic core to assume both a planar (**7a**) and chair (**7c**) conformation nicely demonstrates the ability to tune the conformational nature of these synthons via changes in pendant functionality.

Results and Discussion

Synthesis. Initial synthetic efforts focused on the construction of the desired macrocycles based on isopropylidene subunits, as outlined in Scheme 1. 3,5-Diethynyl pyridine[11] was cross-coupled[12] via palladium-catalysis with 2 equiv of the readily available building block vinyl triflate **2a**[13] to give the product **3a** in 79% yield. Deprotection of the trimethylsilyl-protected acetylenes of **3a** was achieved by treating with methanolic K_2CO_3. The resulting tetrayne **4a** was then carried on, after an aqueous workup, to an intermolecular oxidative acetylenic homocoupling reaction[14] via treatment with CuI and TMEDA at high dilution in CH_2Cl_2 in the presence of air (Scheme 2).[15] The reaction was stirred at room temperature until TLC analysis indicated the absence of all of the starting tetrayne **4a** (ca. 1.5 h).

Scheme 1

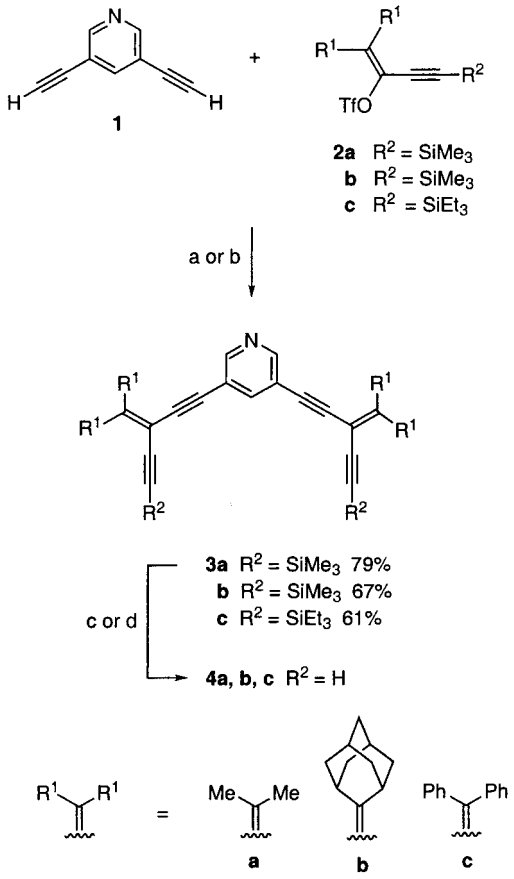

Reagents and conditions: (a) $Pd(PPh_3)_4$, CuI, Et_2NH, THF, rt (for **2a–b**); (b) $Pd(PPh_3)_4$, CuI, Et_2NH, THF, 55 °C (for **2c**); (c) K_2CO_3, wet MeOH/THF, rt; (d) TBAF, THF, rt.

Following aqueous workup, the solvent volume was reduced to afford a solid mixture containing **5a** and what was presumed to be oligomeric byproducts. This mixture was extremely insoluble in organic solvents, making column chromatography impractical. As well, all attempts to selectively extract **5a** from this mixture were unsuccessful. When the mixture was treated with 2 equiv of porphyrin **6a** (based on **3a**), however, TLC analysis (alumina) clearly indicated the formation of only one product. Furthermore, coordination to the porphyrin resulted in vastly increased solubility. This allowed for the isolation of assembly **7a** as a dark red solid, in 39% yield (from **3a**), via column chromatography on neutral alumina. Excess porphyrin remaining from the reaction can be easily recovered by flushing the column with $EtOH/CH_2Cl_2$, following the isolation of **7a**. While pure **7a** shows limited stability under ambient conditions, it can be stored indefinitely under refrigeration. Thermally, the assembly **7a** decomposes at 132 °C.

We then focused on modifying the vinylidene substitution, intending to improve both the solubility and stability of the macrocyclic ligand. Adamantylidene-substituted vinyl triflate **2b**[16] was cross-coupled to **1** to give tetrayne **3b** in 67% yield. Following deprotection, the product **4b**

(9) Maiya, B. G.; Bampos, N.; Kumar, A. A.; Feeder, N.; Sanders, J. K. M. *New J. Chem.* **2001**, 797−800. Chichak, K.; Branda, N. R. *Chem. Commun.* **2000**, 1211−1212. Haycock, R. A.; Hunter, C. A.; James, D. A.; Michelsen, U.; Sutton, L. R. *Org. Lett.* **2000**, *2*, 2435−2438. Hunter, C. A.; Hyde, R. K. *Angew. Chem., Int. Ed. Engl.* **1996**, *35*, 1936−1939. Hunter, C. A.; Shannon, R. J. *Chem. Commun.* **1996**, 1361−1362. Hunter, C. A.; Sarson, L. D. *Angew. Chem., Int. Ed. Engl.* **1994**, *33*, 2313−2316. Fleischer, E. B.; Shachter, A. M. *Inorg. Chem.* **1991**, *30*, 3763−3769.

(10) Mongin, O.; Hoyler, N.; Gossauer, A. *Eur. J. Org. Chem.* **2000**, 1193−1197. Ogawa, K.; Kobuke, Y. *Angew. Chem., Int. Ed.* **2000**, *39*, 4070−4073. Anderson, H. L. *Chem. Commun.* **1999**, 2323−2330. Vicente, M. G. H.; Jaquinod, L.; Smith, K. M. *Chem. Commun.* **1999**, 1771−1782. Fan, J.; Whiteford, J. A.; Olenyuk, B.; Levin, M. D.; Stang, P. J.; Fleischer, E. B. *J. Am. Chem. Soc.* **1999**, *121*, 2741−2752. Drain, C. M.; Nifiatis, F.; Vasenko, A.; Batteas, J. D. *Angew. Chem., Int. Ed.* **1998**, *37*, 2344−2347. Wagner, R. W.; Seth, J.; Yang, S. I.; Kim, D.; Bocian, D. F.; Holten, D.; Lindsey, J. S. *J. Org. Chem.* **1998**, *63*, 5042−5049.

(11) Ng, S. C.; Novak, I.; You, X.; Huang, W. *J. Phys. Chem. A* **1998**, *102*, 904−908.

(12) (a) Zhao, Y.; Tykwinski, R. R. *J. Am. Chem. Soc.* **1999**, *121*, 458−459. (b) Zhao, Y.; Campbell, K.; Tykwinski, R. R. *J. Org. Chem.* **2002**, *67*, 336−344.

(13) Stang, P. J.; Fisk, T. E. *Synthesis* **1979**, 438−440.

(14) Siemsen, P.; Livingston, R. C.; Diederich, F. *Angew. Chem., Int. Ed.* **2000**, *39*, 2632−2657.

(15) Hay, A. S. *J. Org. Chem.* **1962**, *27*, 3320−3321.

(16) Stang, P. J.; White, M. R.; Maas, G. *Organometallics* **1983**, *2*, 720−725.

Scheme 2

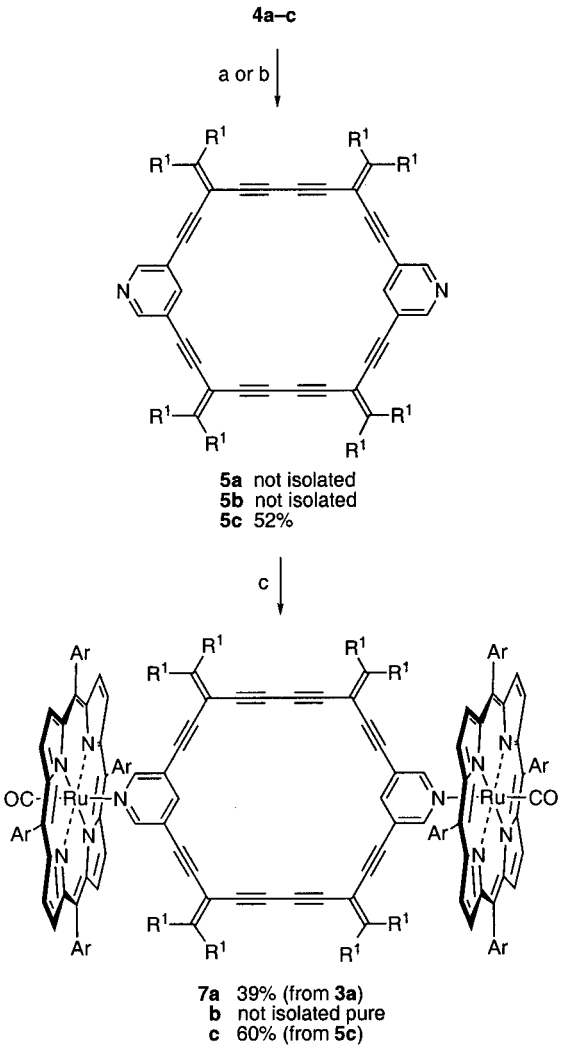

Reagents and conditions: (a) CuI, TMEDA, O_2, CH_2Cl_2, rt (for **4a** and **4c**); (b) CuCl, DBU, mol. sieves, pyridine, O_2, rt (for **4b**); (c) **6a** (2 equiv.), CH_2Cl_2, rt.

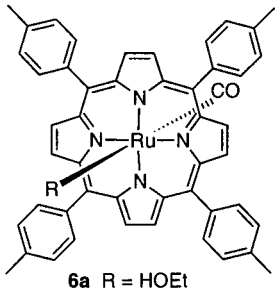

was subjected to standard oxidative coupling conditions. Surprisingly, none of the anticipated macrocyclic product **5b** was observed. Instead, the only isolated product was the iodinated oligomer, **8** (eq 1). This product is presumably formed via reductive elimination across a Cu(II) species to yield the alkynyl iodide. Attempts to perform the analogous homocoupling reaction of **4b** using CuCl catalyst were then targeted. After monitoring the reaction for 5 days, however, TLC analysis still revealed the presence of a significant amount of the starting material, **4b**, even after bubbling O_2 through the reaction mixture. As oxidative coupling reactions are often favored by a strong base and rigorously anhydrous reaction conditions,[14] our strategy was again modified. Oxygen was vigorously bubbled through a solution of **4b**, CuCl, and DBU in pyridine over molecular sieves for 14 h. After aqueous workup, ^{1}H NMR and mass spectral analysis of the crude product revealed the presence of the protonated macrocyclic product **5b**. Unfortunately, all attempts to isolate the pure, deprotonated macrocyclic product **5b** were unsuccessful. As a result, porphyrin **6a** was added to the crude reaction mixture, following treatment with base, in an attempt to mediate the purification process. ESI MS revealed the presence of the desired assembly product **7b**, but all efforts to purify **7b** via recrystallization and chromatography were unsuccessful. While further efforts would likely allow for the isolation of **5b** and the corresponding assembly **7b**, this synthesis produced such low yields of the desired product that such efforts were considered to be impractical.

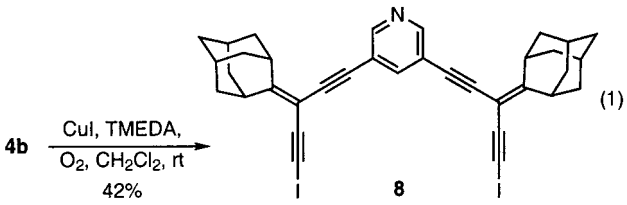

The next modification to the synthesis was to incorporate diphenyl vinylidene functionality, accessible from vinyl triflate **2c**. It was anticipated that the diphenyl vinylidene substitution would impart greater solubility and stability to the system,[17] facilitating purification and characterization. Diethynyl pyridine **1** was cross-coupled to **2c** to give the polyyne **3c** in 61% yield. In contrast to **2a**,**b**, the chemically more robust triethylsilyl protecting group was necessary to ensure the stability of vinyl triflate **2c** during synthesis and purification. Desilylation of **3c** was effected by treatment with TBAF in wet THF. This afforded the deprotected tetrayne **4c**, which was subjected to intermolecular homocoupling conditions (CuI/TMEDA in CH_2Cl_2, in the presence of air). After the addition of ether to the reaction mixture, washing with saturated aqueous NH_4Cl, and drying, the solvent was reduced by about 80%, leading to the formation of a bright yellow precipitate. This solid was filtered and dried to give pure **5c** in 51% yield. It is worth noting that pure **5c** has been accessible by this method alone. All attempts to isolate **5c** from the crude reaction mixture after evaporation of the solvent have been unsuccessful. As with macrocycle **5a**, the crude reaction mixture is quite insoluble and, therefore, difficult to purify by column chromatography. Likewise, attempts to resolvate the crude reaction mixture and then recrystallize **5c** have been equally unsuccessful. While the ligand **5c** is only marginally soluble (<2 mg/mL in CH_2Cl_2), it is quite stable to air, heat, and light, and may be stored for months under refrigeration without observable degradation. It decomposes thermally at temperatures exceeding 170 °C.

The self-assembly reaction of **5c** with porphyrin **6a** was performed in CH_2Cl_2. The addition of 2 equiv of porphyrin **6a**, followed by recrystallization from CH_2Cl_2, allowed for

(17) Decomposition of **5a** and **7a** likely results from an oxygen ene reaction at the isopropylidene protons; see ref 12b.

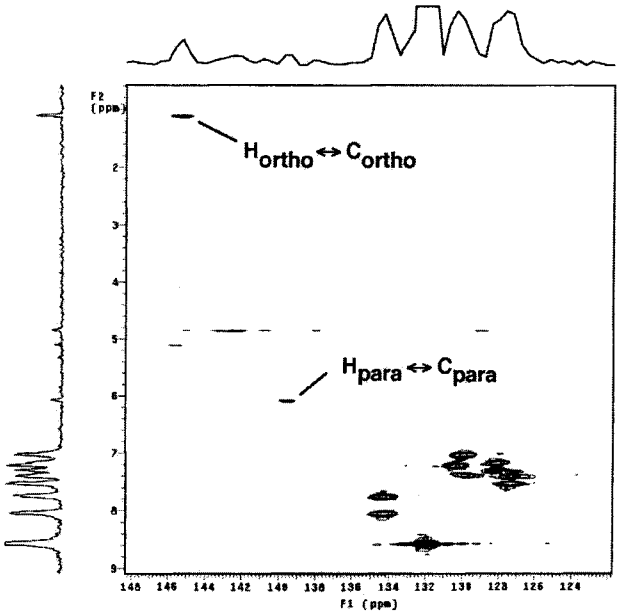

Figure 2. gHMQC NMR spectrum for **7c** (in CD_2Cl_2) showing correlations for the ortho and para pyridyl protons.

isolation of the desired assembly **7c**, a bright red solid, in 60% yield. The progress of the assembly reaction was also monitored by ^{1}H NMR spectroscopy. Aliquots of **6a** were slowly added to a dilute solution of **5c** in CD_2Cl_2, resulting in the formation of the assembly product **7c**. While the reaction appears to proceed quantitatively on the basis of NMR analysis, the moderate isolated yield is apparently due to the weaker association of complex **7c** in solution (in comparison to the isopropylidene-functionalized analogue, **7a**). Unlike **7a**, the macrocyclic portion of **7c** dissociates from the Ru-porphyrins when the complex is subjected to chromatography, with either alumina or silica, regardless of the solvent employed. Attempts to precipitate complex **7c** from a CH_2Cl_2 solution via the addition of other solvents (e.g., hexanes, ether, and toluene) have been unsuccessful. These efforts resulted only in the precipitation of macrocycle **5c** from the solution as a result of dissociation of the axially bound porphyrins from the complex. This behavior of **7c** is in stark contrast to that of complex **7a**, which is stable to chromatography and can be precipitated intact from solution. In the solid state, the complex **7c** is thermally quite stable, decomposing only at >250 °C.

Characterization. The most convincing evidence for the formation of assemblies **7a** and **7c** in solution comes primarily from NMR spectroscopic analysis. In the ^{1}H NMR spectrum of **5c**, the ortho and para pyridyl protons give rise to signals at 8.13 and 7.83 ppm, respectively. Upon assembly with the tetratolylporphyrin **6a**, however, these protons are significantly shielded to δ 1.12 and 6.08, respectively, due to the diamagnetic anisotropy of the porphyrin ring. This effect is quite dramatic for the ortho protons due to their proximity to the porphyrin ring. Similarly, the ^{1}H NMR spectrum of assembly **7a** shows the ortho and para pyridyl proton signals at 1.30 and 6.04 ppm, respectively. Two-dimensional gHMQC NMR analyses for both **7a** and **7c** provided confirmation of these proton assignments. As shown in Figure 2, the signals ascribed to the ortho and para pyridyl protons of **7c** correlate to signals at ca. 145.2 and 139.6 ppm, respectively, on the F1 axis of the spectrum, consistent with the chemical shifts expected for these pyridyl carbons.

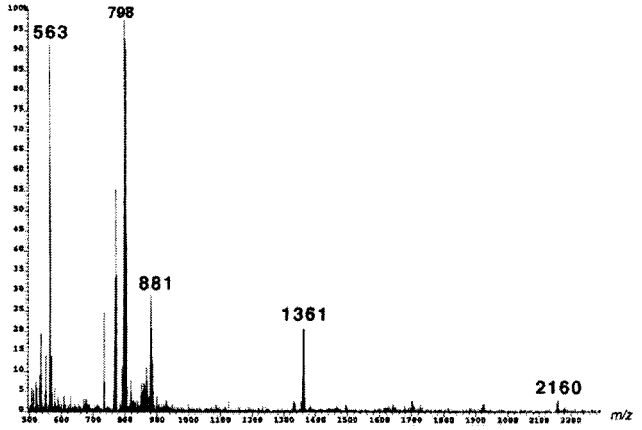

Figure 3. ESI MS (nitromethane) for supramolecular complex **7a**.

The solution-state presence of complexes **7a** and **7c** is also supported by MS analysis. In the ESI mass spectrum of **7a** (nitromethane), a cluster of signals centered at *m/z* 2160 (3% intensity) is observed (Figure 3). Comparison of the calculated and observed isotopic distribution patterns for **7a** suggests that these signals are consistent with a combination of protonated $[M + H]^+$ and radical cation species $[M]^{+\bullet}$. A fragment peak of greater intensity (21%) is observed at *m/z* 1361, resulting from the loss of one porphyrin unit. The isotopic distribution of this peak also suggests the presence of both the radical cationic and protonated species. Other significant fragments include peaks at *m/z* 798 (100% intensity, radical cation) corresponding to the porphyrin and at *m/z* 563 (92%) representing the protonated macrocyclic ligand $[\mathbf{5a} + H]^+$. Numerous attempts were made to improve the intensity of the $[M + H]^+$ and/or $[M]^{+\bullet}$ peaks, including varying the applied voltage, using different combinations of solvents, and acquiring the spectra at lower temperatures. All strategies resulted in a loss of sensitivity with no significant gains in intensity.

For the less robust assembly, **7c**, an $[M + H]^+$ signal is not found in the ESI MS. A signal at *m/z* 1856 (3%) is observed, corresponding to the fragment resulting from the loss of one porphyrin moiety. MALDI-TOF analysis has also been employed for **7c**, with 1,8,9-trihydroxyanthracene as the matrix and irradiation at 337 nm. As shown in Figure 4, the most diagnostic signal is found at *m/z* 1829, corresponding to assembly **7c** with the loss of one complete porphyrin moiety as well as the second porphyrinic CO group. As the photochemical dissociation of CO from ruthenium porphyrins is well-known,[18] this fragmentation is not unexpected considering the irradiation wavelength. In addition to the protonated macrocycle at *m/z* 1059.9, signals corresponding to the porphyrin radical cation (*m/z* 770.4) and a porphyrin dimer (*m/z* 1535.2) (where both species are decarbonylated) are also clearly present in the spectrum.

Solid-State Characterization. Single crystals of **7a** suitable for X-ray crystallographic analysis were obtained from a crude reaction mixture containing **7a** and excess porphyrin **6a** in CH_2Cl_2. The complex **7a** cocrystallized

(18) Saito, M.; Endo, A.; Shimizu, K.; Satô, G. P. *Electrochim. Acta* **2000**, *45*, 3021−3028. Funatsu, K.; Kimura, A.; Imamura, T.; Ichimura, A.; Sasaki, Y. *Inorg. Chem.* **1997**, *36*, 1625−1635.

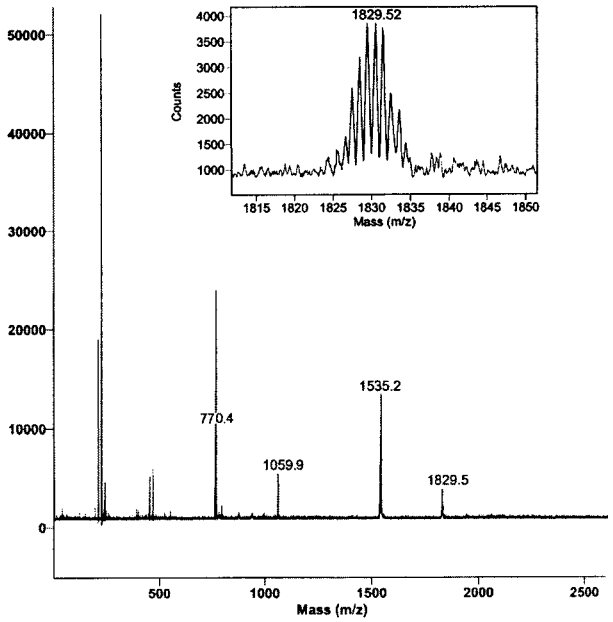

Figure 4. MALDI-TOF spectrum for **7c**.

with 1 equiv of **6a** such that the excess porphyrin is captured between the layers of the assembly product. An ORTEP of **7a** is shown in Figure 5, and the internal dimensions of the macrocycle circumscribed by the enyne scaffold provide a cavity of 0.64 × 1.0 nm. The framework of the macrocyclic core is virtually planar. It also appears to be nearly free from strain, as all alkyne angles are within 8.2° of the expected value of 180° with a mean deviation of 3.6°. Furthermore, the vinylidene bond angles C(77)−C(78)−C(82) and C(85)−C(86)−C(90) at 115.5 and 113.7° are quite similar to those found for analogous acyclic systems.[12]

When the crystal packing for **7a** is viewed along the *b*-axis (Figure 5, bottom), stacking of the macrocyclic portion of the assembly in the solid state can be observed. The majority of the cavity created by organization of the macrocycles is occupied the tolyl groups of two of the offset porphyrin cocrystallites, which are shown in gray (Figure 5). The void space remaining within the unit cell, at 751.6 Å^3, is still rather large and represents 17.4% of the total unit cell volume. This so-called void space is likely to be occupied by solvent, but the final electron density difference map is ambiguous as to the location and/or the identity of the solvent molecules. The layers of the macrocyclic assemblies are separated by approximately 9 Å to accommodate the cocrystallized porphyrin molecules. While single crystals are also available from a CH_2Cl_2 solution of pure **7a**, to date, all attempts at X-ray crystallographic analysis have been hindered by the rapid desolvation of these crystals. Likewise, attempts to cocrystallize **7a** with small molecules that might be suitable for inclusion in the pores of **7a** have also been unsuccessful.

Single crystals of **7c** suitable for X-ray analysis were formed from a CH_2Cl_2 solution of the pure assembly in the presence of *n*-hexadecane. The structure of **7c** incorporates one hexadecane molecule in the unit cell, the presence of which hampered data refinement. Figure 6 shows the ORTEP of the centrosymmetrical **7c** and confirms the coordination of **5c** to the porphyrin in the solid state. Analysis of this solid-state structure reveals that the enyne core of the macrocycle is no longer planar

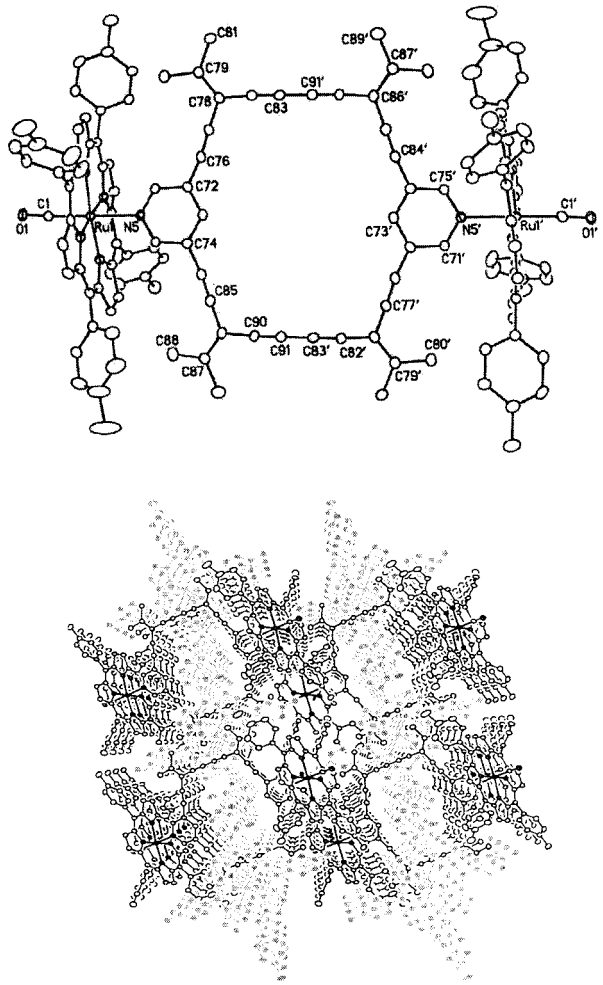

Figure 5. Top: ORTEP drawing of supramolecular assembly **7a** (20% probability level). Bottom: View down the crystallographic *b*-axis showing order within the crystal lattice (cocrystallite porphyrin **6a** shown in gray). Primed atoms are related to unprimed ones by a crystallographic inversion center.

as found for **7a** but instead adopts a chairlike conformation. The degree of distortion can be approximated by measuring the dihedral angles of the three chairs generated in this conformation. Using a dummy atom at the center of the pyridine ring as one vertex (centroid) of the hexagon, and the alkylidene carbons C(78) and C(96) as the others, the following dihedral angles are obtained: (1) 59.3° [(centroid)−C(78)−C(96)−(centroid)′], (2) 61.8° [C(78)−C(96)−(centroid)′−C(78)′], and (3) 64.5° [C(96)−(centroid)′−C(78)′−C(96)′]. This gives an average value of 61.9°, considerably larger than that of cyclohexane at 55.1°.[19] The distortion from planarity is also greater than that of a recently reported expanded radialene, which has an average dihedral angle of 57.2°.[1m] The macrocyclic portion of assembly **7a**, by the same comparison, possesses a mean dihedral angle of only 3.2°. The chair conformation of **7c** results in a reduction of the alkylidene bond angles C(77)−C(78)−C(92) and C(95)−C(96)−C(110), which at 113.6 and 112.3°, respectively, are smaller by 1.8° than those found for precursor **3c**.[20] The remarkable puckering of the macrocyclic core likely

(19) Kahn, R.; Fourme, R.; André, D.; Renaud, M. *Acta Crystallogr. Sect. B* **1973**, *29*, 131−138.
(20) Campbell, K.; Tykwinski, R. R. Unpublished results.

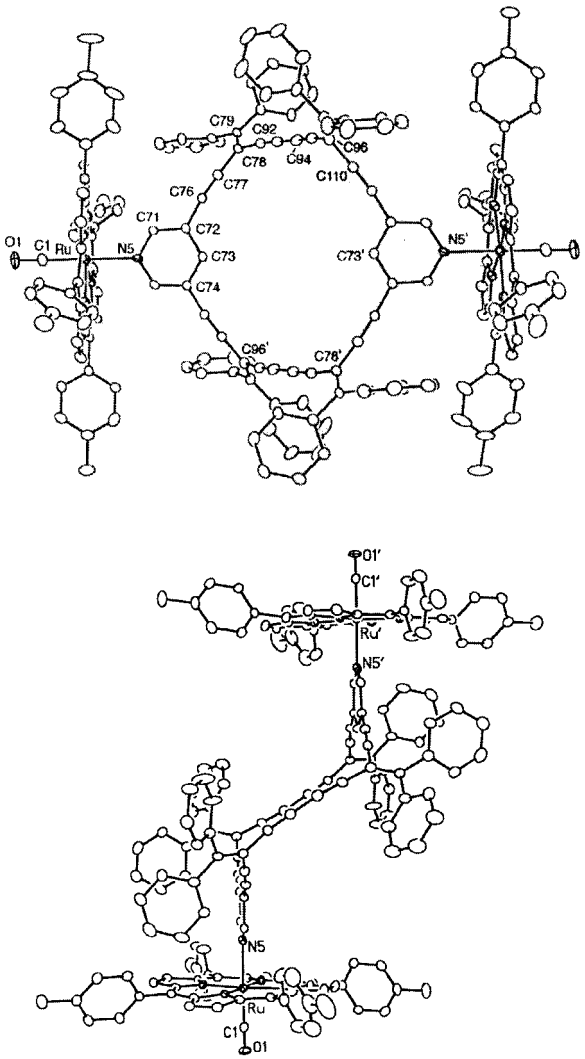

Figure 6. Top: ORTEP drawing of supramolecular complex **7c** (20% probability level, hexadecane removed). Bottom: Alternate view emphasizing the chair conformation of the macrocyclic core. Primed atoms are related to unprimed ones by a crystallographic inversion center.

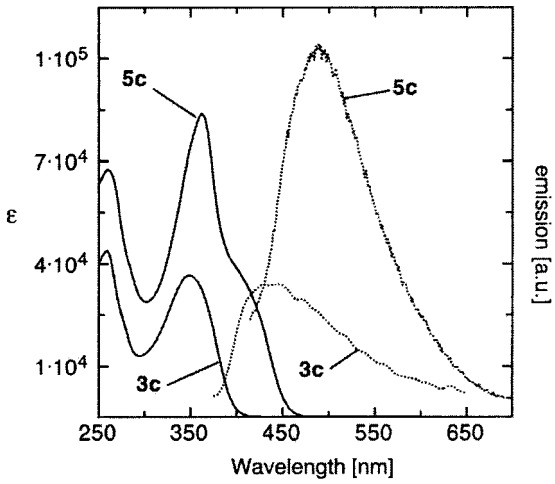

Figure 7. Absorption (solid lines) and emission (broken lines) spectra for **3c** and **5c** (in CH_2Cl_2).

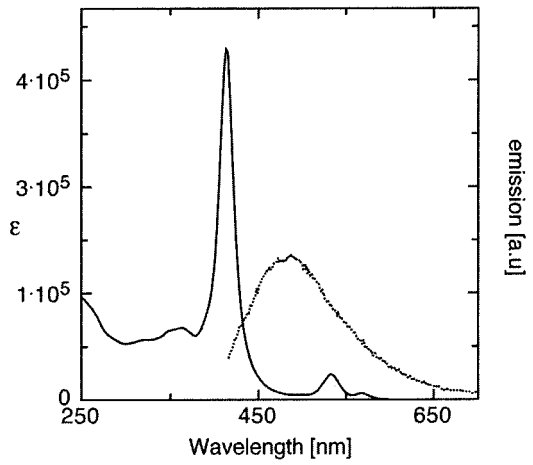

Figure 8. Absorption (solid line) and emission (broken line) spectra for complex **7c** (in CH_2Cl_2).

results from increased steric interactions between the diphenyl vinylidene substitution and the attached porphyrin ring(s). This observation also helps to account for the observed fragility of assembly **7c** in solution in comparison to **7a**. Somewhat surprisingly, however, is that the disparity in chemical stability between **7a** and **7c** is not reflected in N−Ru bond lengths, which are identical within 0.001 Å for both molecules at 2.218 Å.

The apparent flexibility of the macrocyclic ligand of **7c** in the solid state discussed above suggested that, in solution, the interconversion between two degenerate chair conformations (via a twisted or planar intermediate) or between a chair and planar conformation might be feasible. Attempts to explore this possibility have, however, been inconclusive due to the lack of a suitable spectroscopic signature that would indicate a planar or twisted conformation. Variable-temperature ^{1}H NMR spectra obtained over a temperature range of 30 to −80 °C for **7c** showed no significant chemical shift change for any resonance that would suggest that two conformations were in equilibrium in solution.

Electronic Characteristics. The electronic characteristics of assemblies **7a** and **7c**, as well as their components, were analyzed by UV−vis and fluorescence spectroscopies. Whereas structures with dimethyl vinylidene substitution do not show significant fluorescence, the diphenyl vinylidene moiety greatly enhances emissive behavior. As seen in Figure 7, the absorption spectrum for **5c** shows a longer wavelength absorption band, the shoulder centered near 401 nm, as a result of the extended conjugated framework in comparison to precursor **3c** (λ_{max} = 348 nm). The lower energy HOMO−LUMO gap for **5c** is also reflected in the emission spectrum, where the emission maximum for **5c**, centered at 491 nm (excitation at 362 nm), is red-shifted by 45 nm from that of **3c** at 446 nm (excitation at 340 nm).

The absorption spectrum of **7c** is, for the most part, the sum of its component parts, i.e., **5c** + 2 equiv of **6a**. The Soret Band for both complexes **7a** and **7c** is found at 413 nm, identical to the energy of **6a**.[21] The two Q-Band absorptions for complexes **7a** and **7c** found at 569 and 534 nm, however, are slightly red-shifted versus those of **6a** (562 and 530 nm). Assembly **7c** shows an emission at 489 nm (excitation at 364 nm) situated in the region of low molar absorptivity for the porphyrin (Figure 8). Although the emission energy for **7c** is nearly identical to that of the pure macrocycle **5c**, the relative

(21) These spectra are provided as Supporting Information.

emission intensity is greater for **7c**. This fact supports emission from the macrocyclic core of **7c** rather than emission from free **5c** generated from a dissociation equilibrium established in solution. A very weak emission from **7c** can also be observed at ca. 725 nm (not shown). This emission is characteristic of both porphyrin **6a** and **6b** in solution.[22] It is unknown, therefore, whether this low-energy emission results from the porphyrin complexed in **7c**, or from a small concentration of free porphyrin generated via dissociation of **7c** (or from both).

Conclusions

We have described a synthetic route to functionalized macrocycles based on a simple 3,5-diethynyl pyridine building block. The ability of these macrocycles to function as ligands and to participate in self-assembly reactions has been demonstrated, yielding nanoscale assemblies **7a** and **7c**. These assemblies were characterized both in solution as well as in the solid state. Analysis of the solid-state structure of **7a** reveals the ability of these ligands to form highly ordered, channel-like materials. A similar analysis of **7c** reveals that steric interactions impede planarity as the size of the vinylidene substitution is increased from methyl to phenyl. These steric constraints lead to a chairlike conformation for **7c** in the solid state that demonstrates the flexibility of these macrocycles as supramolecular synthons. Future efforts will focus on further exploring the utility of these molecules as ligands in other self-assembly reactions, using less sterically demanding metal fragments.

Experimental Section

General Methods. Reagents were purchased reagent grade from commercial suppliers and used without further purification. 3,5-Diethynyl pyridine,[11] **2a**,**c**,[12] and **2b**[16] were prepared as previously reported. Evaporation and concentration in vacuo was achieved at H_2O-aspirator pressure. Drying was done over anhydrous $MgSO_4$. All Pd-catalyzed coupling reactions were performed in standard, dry glassware under an inert atmosphere of N_2. A positive pressure of N_2 was essential to the success of all Pd-catalyzed reactions. Degassing of solvents was accomplished by vigorously bubbling N_2 through the solutions for greater than 45 min. Column chromatography was performed on aluminum oxide, neutral Brockman 1, or silica gel.

X-ray crystal data for **7a** (Figure 5): ($C_{191}H_{144}N_{14}O_4Ru_3$); M = 3002.41, triclinic space group $P\bar{1}$ (No. 2), ρ_{calcd} = 1.157 g/cm^3, Z = 1, a = 16.1421(11) Å, b = 17.1025(11) Å, c = 17.5359(12) Å, α = 90.3641 (14)°, β = 100.8011 (13)°, γ = 114.5012 (14)°, V = 4308.0 (5) Å^3, μ = 0.316 mm^{-1}. Final $R(F)$ = 0.0887, wR_2 (F^2) = 0.2941 for 960 variables and 17506 data with $F_o^2 \geq -3\sigma(F_o^2)$ (10363 observations [$F_o^2 \geq 2\sigma(F_o^2)$]). Full details can be found in Supporting Information and in ref 4.

X-ray crystal data for **7c** (Figure 6): ($C_{180}H_{118}N_{10}O_2Ru_2 \cdot C_{16}H_{34}$); M = 2881.42, triclinic space group $P\bar{1}$ (No. 2), ρ_{calcd} = 1.022 g/cm^3, Z = 1, a = 13.9983(16) Å, b = 17.099(2) Å, c = 22.220(3) Å, α = 100.949 (2)°, β = 96.942 (2)°, γ = 113.311 (2)°, V = 4680.6 (9) Å^3, μ = 0.211 mm^{-1}. Final $R(F)$ = 0.1079, wR_2 (F^2) = 0.3587 for 958 variables and 18770 data with $F_o^2 \geq -3\sigma(F_o^2)$ (8613 observations [$F_o^2 \geq 2\sigma(F_o^2)$]). Full details can be found in Supporting Information.

General Cross-Coupling Procedure. Two equivalents of the appropriate vinyl triflate, **2a**−**c**, were added to a dry, degassed solution of diethynyl pyridine **1** in THF. $Ph(PPh_3)_4$ (ca. 0.05 equiv) and Et_2NH were added, and the solution was stirred for 5 min. CuI (ca. 0.15 equiv) was added, and the solution was stirred at the temperature indicated until TLC analysis no longer indicated the presence of the polyyne starting material. Ether was added, and the resulting solution was washed with saturated aqueous NH_4Cl (2 × 25 mL) and dried; the solvent was removed in vacuo. Chromatography and/or recrystallization from acetone gave the desired oligomer.

General Homocoupling Procedure. A mixture of the appropriate trimethylsilyl- or triethylsilyl-protected polyyne and K_2CO_3 (ca. 0.2 equiv) or TBAF (ca. 2.2 equiv) in wet THF/MeOH (1:1, 25 mL) or THF (25 mL), respectively, was stirred at room temperature until TLC analysis revealed the disappearance of all trialkylsilyl-protected species. Ether was added, and the resulting solution was washed with saturated aqueous NH_4Cl (2 × 25 mL) and dried. The solvent was reduced to ca. 1 mL, and dry CH_2Cl_2 was added. A solution of CuI (ca. 7 equiv) and TMEDA (ca. 20 equiv) in ca. 10 mL of dry CH_2Cl_2 was prepared and added slowly to the solution containing the deprotected polyyne. The reaction mixture was stirred at the temperature indicated until TLC analysis no longer showed the presence of the deprotected polyyne. Ether was added, and the resulting solution was washed with saturated aqueous NH_4Cl (6 × 75 mL) and dried.

3,5-Bis(1-trimethylsilyl-3-propylidene-1,4-pentadiynyl)-pyridine (3a). Diethynyl pyridine **1** (0.13 g, 1.0 mmol) was cross-coupled with vinyl triflate **2a** (0.63 g, 2.1 mmol) in dry, degassed THF (80 mL) in the presence of $Pd(PPh_3)_4$ (50 mg, 0.040 mmol), CuI (25 mg, 0.13 mmol), and Et_2NH (4 mL) at room temperature for 30 min as described in the general procedure. Flash chromatography on alumina (hexanes/CH_2Cl_2, 2:1) yielded **3a** (0.36 g, 79%) as a colorless solid: mp 71−72 °C; R_f = 0.40 (hexanes/CH_2Cl_2, 2:1); UV−vis (CH_2Cl_2) 297 (30700) nm; IR (μscope) 2959, 2904, 2210, 2151, 1577 cm^{-1}; ^{1}H NMR (300 MHz, $CDCl_3$) δ 8.54 (br s, 2H), 7.78 (br s, 1H), 2.08 (s, 12H), 0.21 (s, 18H); ^{13}C NMR (75.5 MHz, APT, CD_2Cl_2) δ 158.3, 150.9, 140.3, 120.4, 101.2, 101.2, 97.1, 90.2, 87.5, 23.1, 23.0, 0.0; ESI MS (MeOH/toluene) m/z (rel intensity): 428.2 ([M + H]$^+$, 100); ESI HRMS calcd for $C_{27}H_{34}NSi_2$ ([M + H]$^+$) 428.2230, found 428.2226.

3,5-Bis(1-trimethylsilyl-3-adamantylidene-1,4-pentadiynyl)pyridine (3b). Compound **1** (35 mg, 0.28 mmol) was cross-coupled with **2b** (0.19 g, 0.47 mmol) in dry, degassed THF (20 mL) in the presence of $Pd(PPh_3)_4$ (25 mg, 0.020 mmol), CuI (12 mg, 0.060 mmol), and Et_2NH (2 mL) at room temperature for 1 h as described in the general procedure. Purification by column chromatography on alumina (hexanes/CH_2Cl_2 1:1) afforded **3b** (113 mg, 67%) as an off-white solid: mp 181−183 °C; R_f = 0.65 (hexanes/CH_2Cl_2 1:1); UV−vis (CH_2Cl_2) 250 (35600), 305 (32900) nm; IR (μscope) 3037, 2850, 2203, 2152, 1448 cm^{-1}; ^{1}H NMR (300 MHz, CD_2Cl_2) δ 8.53 (d, J = 2.1 Hz, 2H), 7.78 (t, J = 2.0, 1H), 3.30 (s br, 4H), 2.02−1.80 (m, 24 H), 0.22 (s, 18H); ^{13}C NMR (75 MHz, CD_2Cl_2, APT) δ 173.3, 150.7, 140.3, 120.5, 100.7, 96.4, 93.4, 89.8, 87.0, 39.7, 39.6, 37.2, 37.1, 37.0, 28.4, 0.1 (one coincident peak not observed); ESIMS (MeOH/tol 3:1) m/z 612.3 ([M + H]$^+$, 100); ESI HRMS calcd for $C_{41}H_{50}NSi_2$ ([M + H]$^+$) 612.3482, found 612.3482.

3,5-Bis(1-triethylsilyl-3-diphenylvinylidene-1,4-pentadiynyl)pyridine (3c). Compound **1** (70 mg, 0.55 mmol) was cross-coupled with vinyl triflate **2c** (0.50 g, 1.1 mmol) in dry, degassed THF (65 mL) in the presence of $Pd(PPh_3)_4$ (35 mg, 0.030 mmol), CuI (20 mg, 0.10 mmol), and Et_2NH (1.5 mL). The reaction flask was sealed under N_2 and stirred for 24 h at 55 °C. Evaporation of the solvent and flash chromatography on alumina (hexanes/CH_2Cl_2, 2:1) yielded **3c** (254 mg, 61%) as a colorless solid: mp 118−121 °C; R_f = 0.40 (hexanes/CH_2Cl_2, 2:1); UV−vis (CH_2Cl_2) 259 (48800), 348 (41700) nm; IR (μscope) 3081, 2910, 2205, 2151, 1536 cm^{-1}; ^{1}H NMR (300 MHz, CD_2Cl_2) δ 8.30 (d, J = 2.0 Hz, 2H), 7.33−7.51 (m, 21H), 0.95 (t, J = 7.8 Hz, 18H), 0.60 (q, J = 7.8 Hz, 12H); ^{13}C NMR (75.5 MHz, APT, CD_2Cl_2) δ 158.6, 151.0, 140.6, 140.2, 140.0, 130.7, 130.6, 129.3, 129.2, 128.2, 128.1 (2×), 104.0, 101.8, 96.7, 92.8, 87.7, 7.6, 4.5; ESI MS (MeOH/toluene) m/z (rel intensity) 760.4 ([M + H]$^+$, 100); ESI HRMS calcd for $C_{53}H_{54}NSi_2$ ([M + H]$^+$) 760.3795, found 760.3792.

3,5-Bis(1-iodo-3-adamantylidene-1,4-pentadiynyl)pyridine (8). Compound **3b** (0.10 g, 0.16 mmol) was desilylated by treatment with methanolic K_2CO_3 for 1 h as described in

(22) Chichak, K.; Branda, N. R. *Chem. Commun.* **1999**, 523−524.

the general procedure. After aqueous workup, the deprotected polyyne **4b** was treated with CuI (0.20 g, 1.1 mmol) and TMEDA (0.40 mL, 2.6 mmol) in dry CH_2Cl_2 (350 mL) in the presence of air. The reaction mixture was stirred at room temperature for 2 h. Ether was added, and the resulting solution was washed with saturated aqueous NH_4Cl (6 × 75 mL) and dried; the solvent was removed in vacuo. Purification by column chromatography on silica gel (neat CH_2Cl_2) yielded **4d** (49 mg, 42%) as an off-white solid: $R_f = 0.35$ (silica, CH_2Cl_2); IR (μscope) 2921, 2851, 2205, 1703, 1575 cm^{-1}; ^1H NMR (300 MHz, CD_2Cl_2) δ 8.53 (d, $J = 2.1$ Hz, 2H), 7.78 (t, $J = 2.1$ Hz, 1H), 3.28 (br s, 4H), 1.80−2.03 (m, 24H); ^{13}C NMR (125 MHz, APT, CD_2Cl_2) δ 174.2, 150.6, 140.2, 120.3, 93.6, 89.9, 89.5, 87.3, 39.8, 39.7, 37.1, 37.0, 28.4, 7.8 (two coincident sp^3 peaks not observed); ESI MS (nitromethane) *m/z* (rel intensity): 720.1 ($[M + H]^+$, 100); ESI HRMS calcd for $C_{35}H_{32}NI_2$ ($[M + H]^+$) 720.0624, found 720.0635.

Macrocycle 5a. Oligomer **3a** (0.15 g, 0.36 mmol) was desilylated by treating with methanolic K_2CO_3 for 1 h as described in the general procedure. Deprotected polyyne **4a** was then oxidatively homocoupled in the presence of CuI (0.52 g, 2.7 mmol), TMEDA (1.0 mL, 6.6 mmol), and air in dry CH_2Cl_2 (350 mL) for 90 min at room temperature. After aqueous workup, the solvent was removed under reduced pressure to yield an off-white solid. Macrocycle **5a** was not isolated due to the extremely limited solubility of this crude reaction product.

Macrocycle 5b. Oligomer **3b** (30 mg, 0.049 mmol) was desilylated by treatment with TBAF for 30 min as described in the general procedure. The deprotected polyyne **4b** was then oxidatively coupled in the presence of CuCl (50 mg. 0.51 mmol), DBU (0.50 mL), and O_2 in pyridine (75 mL). The mixture was stirred for 14 h at room temperature. Ether was added, and the resulting solution was washed with saturated aqueous NH_4Cl (4 × 50 mL) and dried. Removal of the solvent yielded the crude macrocycle **5b** that could not be further purified.

Macrocycle 5c. Compound **3c** (82 mg, 0.12 mmol) was desilylated by treatment with TBAF for 30 min as described in the general procedure. Deprotected polyyne **4c** was oxidatively coupled in the presence of CuI (0.18 g, 0.92 mmol), TMEDA (0.35 mL, 2.3 mmol), and air in dry CH_2Cl_2 (220 mL) for 3 h at room temperature followed by 12 h at 4 °C. Following aqueous workup, the solvent was reduced by approximately 80%, resulting in the formation of a bright yellow precipitate. Isolation of the precipitate afforded **5c** (29 mg, 51%) as a bright yellow solid that was not sufficiently soluble for meaningful ^{13}C NMR analysis; mp 172 °C dec; UV−vis (CH_2Cl_2) 260 (72600), 362 (88900), 401 (sh, 43400) nm; IR (μscope) 3052, 2210, 1583, 1513 cm^{-1}; ^1H NMR (300 MHz, CD_2Cl_2) δ 8.13 (d, $J = 1.9$ Hz, 4H), 7.83 (t, $J = 1.9$ Hz, 2H), 7.31−7.48 (m, 40H); ESI MS (MeOH/toluene) *m/z* (rel intensity) 1059.4 ($[M + H]^+$, 43); ESI HRMS calcd for $C_{82}H_{47}N_2$ ($[M + H]^+$) 1059.3734, found 1059.3738.

Macrocyclic Porphyrin Assembly 7a. The crude product mixture containing macrocycle **5a** (0.16 g) was added to a solution of Ru porphyrin **6a** (0.20 g, 0.25 mmol, 2 equiv on the basis of **3a**) in CH_2Cl_2 (2 mL). Flash chromatography on alumina (hexanes/CH_2Cl_2, 1:1) yielded **7a** (0.15 g, 39% overall from **3a**) as a burgundy solid: mp 132 °C dec; UV−vis (CH_2Cl_2) 295 (130900), 414 (519400), 534 (42800); IR (μscope) 3126, 2866, 2210, 1916, 1806, 1575 cm^{-1}; ^1H NMR (300 MHz, CD_2Cl_2) δ 8.64 (s, 16H), 8.11 (dd, $J = 7.8$, 1.9 Hz, 8H), 7.90 (dd, $J = 7.8$, 1.9 Hz, 8H), 7.57 (d, $J = 7.8$ Hz, 8H), 7.46 (d, $J = 7.8$ Hz, 8H), 6.04 (t, $J = 1.7$ Hz, 2H), 2.70 (s, 24H), 2.00 (s, 12H), 1.84 (s, 12H), 1.30 (d, $J = 1.9$ Hz, 4H); ^{13}C NMR (125.3 MHz, CD_2Cl_2) δ 181.1 (C≡O), 161.0, 145.1, 144.0, 139.8, 137.8, 137.4, 134.4 (2×), 132.1, 127.6, 127.3, 122.0, 118.1, 99.7, 88.8, 85.5, 78.1, 75.7, 23.5, 23.2, 21.5; ESI MS (nitromethane) *m/z* (rel intensity) 2160 ($[M + H]^+$, 3), 1361 ($[M - \text{porphyrin}]^+$, 21), 798 ($[\text{porphyrin}]^+$, 100), 563 ($[\mathbf{5a} + H]^+$, 92).

Macrocyclic Porphyrin Assembly 7c. Macrocycle **5c** (10 mg, 0.0090 mmol) was added to a solution of Ru porphyrin **6a** (15 mg, 0.019 mmol) in CH_2Cl_2 (2 mL), and the assembly product crystallized upon concentration to give **7c** (15 mg, 60%) as a bright red solid; mp 266 °C dec; UV−vis (CH_2Cl_2) 363 (101200), 413 (493200), 533 (36000), 568 (9200) nm; IR (μscope) 3021, 1949, 1529, 1512, 1493 cm^{-1}; ^1H NMR (300 MHz, CD_2Cl_2) δ 8.58 (s, 16H), 8.05 (d, $J = 7.7$ Hz, 8H), 7.76 (d, $J = 7.7$ Hz, 8H), 7.53 (d, $J = 7.7$ Hz, 8H), 7.02−7.43 (m, 48H), 6.08 (br s, 2H), 2.65 (s, 24H), 1.12 (br s, 4H); ^{13}C NMR (125.3 MHz, APT, CD_2Cl_2) δ CO peak not observed, 160.4, 145.3, 143.9, 139.8, 139.6, 139.0, 137.3, 134.5, 134.4, 132.1, 130.5, 130.1, 129.7, 128.3, 128.2, 127.6, 127.5, 117.6, 99.2, 90.5, 85.4, 81.3, 76.4, 21.5 (one broad sp^2 CH not observed, one coincident sp^2 CH not observed); ESI MS (nitromethane) *m/z* (rel intensity): 1856 ($[M + H - \text{porphyrin}]^+$, 4), 1059 ($[\mathbf{5b} + H]^+$, 34), 770 ($[\mathbf{6a} - CO]^+$, 100); MALDI MS: 1829 ($[M + H - \text{porphyrin} - CO]^+$).

Acknowledgment. Financial support for this work has been provided by the University of Alberta, the Alberta Science, Research and Technology Authority, and NSERC. We would like to thank Dr. Angelina Morales-Izquierdo for help with the ESI MS and Dr. Tom Nakashima for help with all two-dimensional NMR analyses. We also appreciate helpful discussions with Dr. Neil R. Branda.

Supporting Information Available: ^1H and ^{13}C NMR spectra for compounds **3a**−**c**, **4d**, and **7a**,**c**, ^1H NMR spectra of **5c** and **6**, gHMQC spectra of compounds **7a**,**c**, ESI MS spectra of compounds **7a**, UV−vis analysis for compound **7c** versus (**5c** + 2 equiv **6a**) and compound **7a** versus **7c**, and X-ray crystallographic data for compounds **7a** and **7c**. This material is available free of charge via the Internet at http://pubs.acs.org.

JO0159744